Human TECHNOLOGY

ISSN: 1795-6889

https://ht.csr-pub.eu Volume 18(1), June 2022, 29-44

VR-ORIENTED EEG SIGNAL CLASSIFICATION OF MOTOR IMAGERY TASKS

Stanisław Zakrzewski
Institute of Information Technology
Lodz University of Technology
Poland

Bartłomiej Stasiak
Institute of Information Technology
Lodz University of Technology
Poland

Tomasz Klepaczka
Institute of Information Technology
Lodz University of Technology
Poland

Adam Wojciechowski
Institute of Information Technology
Lodz University of Technology
Poland

Abstract: *Virtual Reality (VR) combined with near real-time EEG signal processing can be used as a supplement to already existing rehabilitation techniques, enabling practitioners and therapists to immerse themselves into a virtual environment together with patients. The goal of this study is to propose a classification model along with all pre-processing and feature extraction steps, which would be able to produce satisfying results while maintaining near real-time performance. The proposed solutions are tested on an EEG signal dataset containing left/right-hand motor imagery movement experiments performed by 52 subjects. Performance of different models is measured using accuracy scores and execution time both in the testing and the training phase. In conclusion, one model is proposed as optimal given the requirements of potential patient rehabilitation procedures.*

Keywords: *real-time EEG analysis, Virtual Reality, CSP filtering, motor imagery.*

DOI: https://doi.org/10.14254/1795-6889.2022.18-1.3

INTRODUCTION

The concept of a brain-computer interface (BCI), which enables users to communicate and interact with the environment, bypassing the normal somatosensory pathways, dates back to the late 1970s. Since then, it has been significantly developed both in terms of signal acquisition methods and potential application areas. The acquisition methods include invasive approaches – in which the electrodes are surgically implanted either above the cortex (electrocorticography, ECoG) or directly in the grey matter of the brain – and non-invasive ones. The latter methods, including most prominently the electroencephalography (EEG), typically suffer from reduced spatial resolution and poor signal-to-noise ratio. Despite this, EEG is currently the most widespread signal source used in a range of BCI applications.

One of the important application areas, as far as EEG-based brain-computer interface is concerned, is motor imagery task recognition and classification. Mental simulation of the physical movements of body parts (Decety, 1996) involves imagined activation of muscle groups without their actual activation. It is employed, for example, in sport and music training, but also as an important part of the neurorehabilitation process in several medical conditions involving motor deficits, such as multiple sclerosis and stroke.

Integrating BCI with immersive virtual reality (VR) environments is a particularly interesting research area that creates opportunities for enabling post-stroke patients to control the virtual representation of the paralyzed limb, which may lead to increased stimulation, motivation for training and enhanced rehabilitation outcomes (Wojciechowski, Wiśniewska, Pyszora, Liberacka-Dwojak, & Juszczyk, 2021).

Successful VR-BCI integration requires solutions to several technical problems, including the choice of the equipment for EEG signal acquisition and virtual reality simulation that would correctly operate in terms of physical characteristics, electromagnetic compatibility, etc. The most critical parameters or – more precisely – evaluation measures that must be considered are accuracy of motor imagery task classification and processing time. The first element is especially important, as due to the generally low quality and poor resolution of the input EEG signal statistical and machine learning approaches are typically used here to reliably extract the target information (Opałka, Stasiak, Szajerman, & Wojciechowski, 2018; Zhang, Yan, & Gong, 2017). Processing time, on the other hand, also cannot be neglected, as the real-time operation is a *sine qua non* condition in all practical VR applications, significantly influencing the user's experience and the sense of immersion.

In this work, we present a study on EEG-based motor imagery task classification for potential applications in a virtual reality environment targeted at post-stroke neurorehabilitation support. Several design principles and configurations of the feature-extraction/classification process are investigated, including electrode and frequency band selection, signal preprocessing methods and the choice of the classifier. Common spatial pattern (CSP) was selected as the primary tool for data dimensionality reduction and feature extraction. The obtained results enabled us to formulate some important and practically useful conclusions regarding the design of the consecutive processing stages and appropriate parameter settings.

BASIC CONCEPTS AND PREVIOUS WORK

The history of brain-computer interfaces (BCI) starts with the first observations of the spontaneous brain electrical activity and – most prominently – with the acquisition of the first human EEG signal, recorded by Hans Berger in 1924 (Haas, 2003). The general idea and the term "brain-computer interface" itself were proposed by Jacques Vidal (1973, 1977). Along with the technological development of devices and signal processing methods, new application areas emerged, including BCI-based video games (Kaplan, Shishkin, Ganin, Basyul, & Zhigalov, 2013; Liao, Chen, Wang, Chen, Li, Chen, Chang, & Lin, 2012; Van de Laar, Gurkok, Bos, Poel, & Nijholt, 2013) and interaction support in virtual reality environments (Cattan, Andreev, & Visinoni, 2020; Lécuyer, Lotte, Reilly, Leeb, Hirose, & Slater, 2008). User interaction typically involves one of the three dominant BCI paradigms: steady-state-visually-evoked-potentials (SSVEP), P300 event-related potentials (ERP), and mental imagery (Cattan et al., 2020). From our point of view, only the latter case is of interest, as it involves voluntary action of the user, without the need for specific stimulus preparation, such as e.g. oscillatory patterns used in SSVEP. The P300 wave (ERP), although not targeted directly in our research, is however of some interest to us, as it appears in response to visual stimulation used during the data collection procedure. ERP is best described as time-locked changes in the activity of neuronal populations in response to a sensory, motor or cognitive event (Pfurtscheller & Da Silva, 1999). This evoked activity, or signal of interest, has a fixed time delay to the stimulus. Locking ERP in time allows extraction of stimuli-related brain activity in the form of EEG signal data. For VR-based applications, ERPs will typically be induced by visual or auditory stimuli. An immersive VR environment ensures that no additional stimuli (i.e. not generated by the VR itself) will be present. Finding potential ERPs in the EEG signal acquired during experiments in the virtual environment can be used as a base to create a BCI capable of classifying brain activity. From the technical point of view, two important subtypes of the ERP phenomenon may be distinguished: Event-Related Desynchronization (ERD) and Event-Related Synchronization (ERS).

Event-Related Desynchronization can be defined as decreased synchrony of the underlying neuronal populations. The exact phenomena behind it are a series of transient postsynaptic responses of main pyramidal neurons triggered by a specific stimulus. It can be observed as power decrease in the signal of the electrode over a given neuronal population.

During hand movement, contralateral desynchronization can be observed in the upper *alpha* (*mu*) band (in the range of about 10-12Hz) close to the hand sensorimotor area. This ERD is present in nearly every subject and can reliably be used in classification tasks. Another contralateral ERD can be observed in lower *beta* (in the range of about 20-24Hz) in a similar location to the *mu* band ERD, only slightly anterior. These ERDs will not be present after performing of the task is stopped.

Event-Related Synchronization occurs when synchrony of the underlying neuronal populations increases. Similarly to the ERD, it can be considered as a series of transient postsynaptic responses of main pyramidal neurons triggered by a specific stimulus and it can be observed as a power increase in the signal of the electrode over a given neuronal population.

ERS is usually associated with the rest state of neuronal populations. ERS behaviour can be described as antagonistic to ERD. While observing contralateral ERD in the *beta* band (18-26Hz) in motor or motor imagery tasks we can also observe ipsilateral ERS in the same band. Furthermore, while performing self-paced hand movements in which *mu* band ERD can be observed, *alpha* band ERS in the occipital area occurs. Another ERS with a relatively good signal-to-noise ratio is post-movement *beta* ERS which can be observed in the corresponding sensorimotor area in the first second after the termination of a voluntary movement while *mu* band ERD is still present.

In the rest of this paper, we consider a problem of EEG signal classification involving three classes (rest state, left-hand motor imagery and right-hand motor imagery). We decided to target hand imagery movement over e.g. left/right foot movement, because neuron populations in the motor cortex areas related to hand movements are larger, hands can perform a higher variety of movements and visualization of hands is easier in a VR environment.

METHODS

Electrode selection

The choice of the appropriate location for the EEG electrodes is particularly important and not straightforward, especially while targeting higher-order cognitive processes or emotional state recognition (Dura & Wosiak, 2021). In our case, however, the area of interest is clearly defined as the primary motor cortex, although the potential benefits of using a broader selection of EEG channels are also considered, as stated below.

It should also be noted that both VR and BCI devices are mounted on the user's head, which may potentially cause some compatibility issues. VR headsets usually come with a head strap that goes around the head just over the ears. Some of these devices have additional support straps connected either to the VR device and the middle of the main strap (i.e. in the median plane) or to the main strap near the ears running parallel to the VR headset (i.e. in the frontal plane). The latter setting may impose some compatibility problems when used along with the BCI interface, as the additional strap (if it cannot be removed) covers the area coincident with the motor cortex.

Two EEG electrodes that are located directly in the areas of the main activity during motor imagery hand movements are C3 and C4 (Fig. 1). We decided to test 4 sets of electrodes:

- 2 channel configuration including C3 and C4, marked by red dots in Fig. 1;
- 10 channel configuration including FC3, C5, C3, C1, CP3, FC4, C2, C4, C6, and CP4, marked as red and green dots in Fig. 1;
- 18 channel configuration including FC5, FC3, FC1, C5, C3, C1, CP5, CP3, CP1, FC2, FC4, FC6, C2, C4, C6, CP2, CP4 and CP6, marked by red, green and blue dots in Fig. 1;
- 64 channel configuration including all 64 available channels. This configuration includes all the electrodes in Fig. 1.

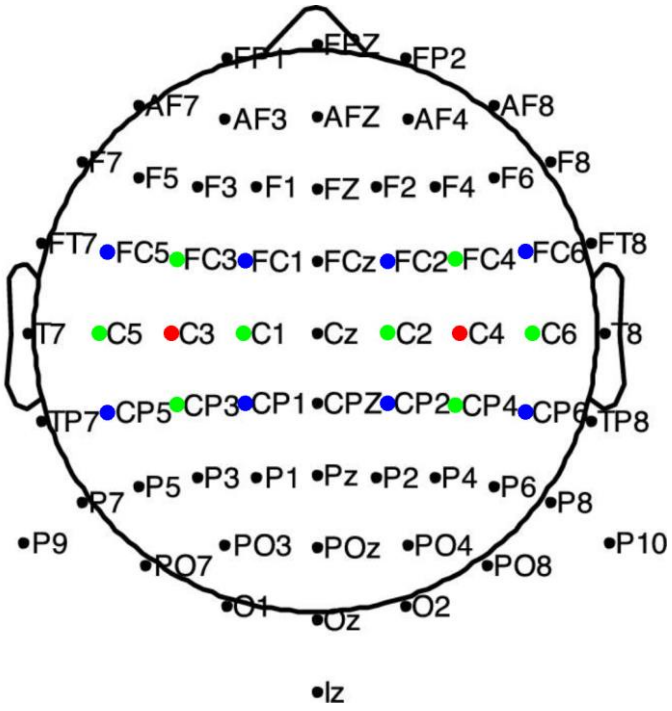

Figure 1. Biosemi64 configuration of EEG electrodes with selected channels highlighted.

The first set is meant to represent the bare minimum to attempt the motor imagery classification task. The second and the third sets represent configurations of electrodes that allow wearing both BCI and VR devices. The last set is used to show how the task can be performed without constraints imposed by the VR headset mount. It should be noted, however, that selecting too many channels can negatively affect near real-time performance which is expected from BCI.

High-pass and band-pass filtering

EEG data is prone to be affected by drifts as it is a recording of electrical activity. To remove these drifts, a high-pass filter with a cutoff frequency of 1Hz is used. Then we apply a band-pass filter with a lower cut-off frequency of 6Hz and a higher cut-off frequency of 30Hz. Frequencies lower than 6Hz are below *mu* band (apart from toddlers that can have *mu* band as low as 5.4Hz but they are not in the subject group) and frequencies higher than 30Hz (upper limit of *beta* waves) do not carry any valid information from our point of view. It is also worth noting that stationary 50/60Hz powerline background frequency, which highly influences any electrical activity recordings, is far above the 30Hz cutoff. Apart from this 6-30Hz filtering, the experiments described in the following sections apply additional band-pass filtering if necessary.

Re-referencing algorithms

EEG recordings are usually performed using a common reference placed somewhere on the head. Some of the possible placements include e.g. vertex (CZ) or linked-ears. We can also omit using the referencing electrode and use one of many existing reference-free techniques. In our research, we use a reference-free method called Common Average Reference (CAR), as it is suitable for all chosen channel configurations. We can apply CAR by removing the mean of all the electrodes from each EEG channel. An example of CAR calculation for the C3 channel (in 10 channel configuration) is shown in Eq. (1).

$$C3_{(CAR)} = C3 - \frac{FC3+C5+C3+C1+CP3+FC4+C2+C4+C6+CP4}{10} \quad (1)$$

For any other configuration, involving a different number of EEG channels, CAR is computed in a similar way.

Common Spatial Pattern filtering

CSP filtering is one of the most frequently used feature extraction algorithms in EEG data binary classification tasks (Alhaddad, 2012). It transforms a band-pass filtered EEG signal into a spatially filtered space. The goal of this transformation is to maximize the individual output signal variance for one class while minimizing it for another class. In fact, the CSP output consists of the same number of channels as the original input signal, but they are sorted by the variance ratio between the two classes. In this way, a low-dimensional linear subspace maximizing the variance ratio may easily be defined and used instead of the original space spanned by all EEG channels. In our approach, the average power of each CSP filter is calculated to obtain an *n*-dimensional feature vector, where *n* is the number of CSP filters.

When ERS occurs in a signal, increased signal variance can be observed. On the other hand, ERD will cause desynchronization of the signal, thus reducing the variance. As the main principle of the CSP filter is to maximize the variance for one class and minimize it for the other, both ERS and ERD play a crucial role here, constituting jointly the fundamental mechanism underlying the actual effectiveness of the CSP-based feature extraction.

CSP has been initially proposed for a two-class scenario. This poses a challenge for classification involving three classes (rest, imagery movement left, imagery movement right). One possible solution would be to split the classification problem into two subproblems, solved by two classifiers consecutively. The first classifier would distinguish between the rest class and imagery movement class and the latter class would be further classified by the second classifier making decision between left and right imagery hand movement. Another solution would be to use multiclass CSP filters. Such a multiclass filter was proposed by Grosse-Wentrup and Buss (2008).

It should be noted that CSP can only be used to reduce the dimensionality of the original signal space. There cannot be more CSP channels than signal sources (electrodes). Therefore, in 2 channel configuration, we use both available output CSP channels (no dimensionality reduction), while in the other configurations (10, 18 and 64 channels) we are using the fixed number of 10 CSP filters with the highest variance ratio.

Hierarchical model

Three-class classification problem cannot be directly solved using a binary CSP – hence, a hierarchical approach was applied. The first step was to classify whether the analysed signal comes from the rest state or an imagery movement (left and right imagery movements combined into one class). When the rest state was detected, it was returned as a result, while an imagery movement needed to be further classified into left or right by another binary classifier. This hierarchical approach can be seen in a diagram in Fig. 2.

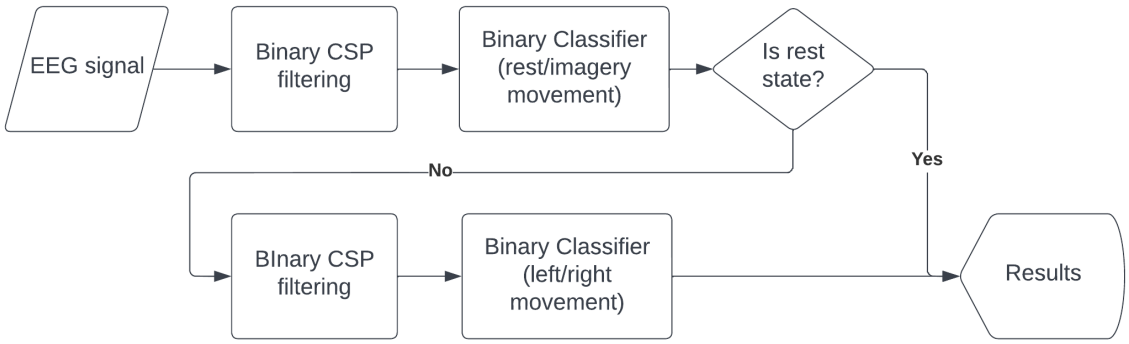

Figure 2. Hierarchical classification workflow for binary CSP filters.

Multiclass model

An alternative implementation of the multiclass CSP filter proposed by Grosse-Wentrup and Buss (2008) simplifies the classification problem, making the hierarchical approach unnecessary. After EEG signal preprocessing with multiclass CSP filters, the classifier is used to label the output data (Fig. 3). In our classification-ready dataset, extracted from an EEG dataset for motor imagery brain–computer interface (Cho, Ahn, Ahn, Kwon & Jun, 2017), the number of the rest state examples is twice the number of either left or right motor imagery examples, as described in the next chapter. A multiclass model working on this whole dataset will be referred to as *multiclass unbalanced*. Another, smaller dataset is derived from our main classification-ready dataset so that the number of the rest state examples is reduced to match the number of left or right imagery movement examples. A model working on this balanced set will be referred to as *multiclass balanced*.

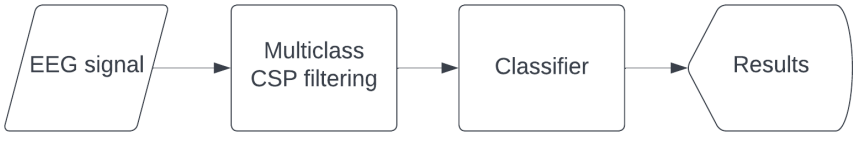

Figure 3. Multiclass classification workflow for multiclass CSP filters.

Classifiers

In our experiments, two popular classifiers were applied: linear discriminant analysis (LDA) and a multilayer perceptron (MLP).

Linear discriminant analysis has also been used by the authors of the original dataset (Cho et al., 2017) for binary classification task (left/right imagery hand movement). LDA searches for a linear combination of predictors that separates two classes in the best way. It is considered a simple yet robust classifier, often able to compete with many more complex methods.

The multilayer perceptron is a powerful non-linear classifier which, as the name suggests, is a neural network with multiple layers of artificial neurons. It may be trained, with appropriate machine learning algorithms, to discover deeply hidden patterns in complex multidimensional input data. It should be noted, however, that in our experiments, the CSP-filtered EEG signals cannot be considered a particularly complex type of data, as the output of each filter is averaged over time, producing just one value (average power) per output CSP channel. In this context, application of the MLP may be seen as a method of comparison and verification of whether the simpler (and faster) LDA is sufficient to perform successful classification in the considered motor imagery task recognition problem.

The MLP classifier used in our experiments was configured to have *n* inputs in the first layer (where *n* is the number of CSP filters applied), 2 hidden layers containing 20 neurons each, with *ReLU* activation function and 3 neurons in the output layer (one for each class). This configuration was selected based on numerous preliminary experiments involving various neural architectures and considering i.a. their training capabilities and generalization properties.

MATERIAL

Motor imagery EEG dataset

We decided to conduct our experiments on a dataset prepared by Cho et al. (2017). This dataset contains EEG signal recordings of 52 healthy subjects performing either motor or motor imagery hand movements (of which we only used the latter ones). Each participant performed 100 or 120 trials for left/right-hand motor imagery movement and each trial lasted around 7 to 8 seconds.

Recording of a single trial begins with 2 seconds of a rest state, then for three seconds an instruction (cue) is shown on a screen, telling the subject to imagine moving left or right hand and finally the instruction disappears from the screen for another 2 seconds of a rest state followed by 0.1 to 0.8 seconds between trials. Trial timeline is shown in Fig. 4.

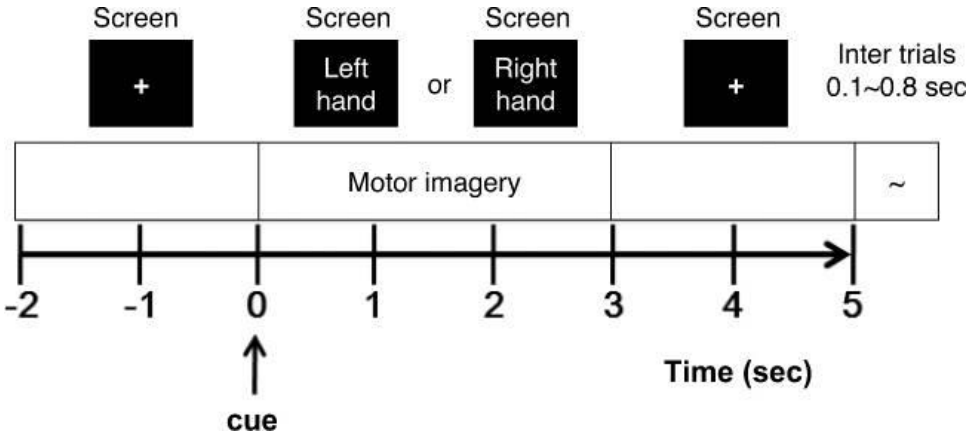

Figure 4. A single trial from the original EEG dataset (Cho, et al., 2017).

EEG signal may be distorted by a variety of artifacts. It is essential to make sure that the data used in classification experiments does not contain too much noise and the high-pass/band-pass filtering used to remove drifts and power line frequency components is just one of the necessary preprocessing steps. Moreover, information about potentially bad trials – as determined by voltage magnitude or correlated with actual muscle activity (EMG) – provided by the authors of the dataset is used. The trials marked as bad are removed from our experiments. It should be noted that it sometimes leads to an imbalance between the classes and for some of the subjects, even up to 90% of their trials are being dropped, which makes the classification task virtually impossible.

To prepare the data for the classification, some additional processing was necessary. Signal splits were extracted from a single trial and assigned an appropriate label. Each trial contains two states, as illustrated in Fig. 2: the rest state and the left/right imagery movement. The rest state split is extracted from the first 2 seconds of a trial recording. We decided not to use the 2 seconds after the imagery movement stops, as this split is likely to be corrupted by both P300 and post imagery movement lower *beta* ERS. To extract imagery movement split, we cut the trial fragment from 0.5 to 2.5 seconds after the instruction appears on the screen. The offset of 0.5s is needed to avoid P300 distortion.

The classification data obtained in this way is not balanced, naturally, as the rest class has twice as many examples as either of the imagery movement data. This imbalance may be an issue in multiclass classification, but it poses no problem in hierarchical classification because in the first classification step (binary classification of rest and imagery movement), the instances of left and right imagery movement are combined into one class.

EXPERIMENTS

Two metrics employed during the experiments were: classification accuracy and runtime. Neither of these should be considered significantly more valuable for VR applications, so in practice, the most optimal combination of accuracy score and runtime should be searched for.

The dataset, described in the previous chapter, is used in a 10-fold cross-validation scheme (train - test ratio: 80% - 20%). As mentioned before, the multiclass balanced model

structure required reducing the number of the rest state examples, which was done before generating the classification data. This classification-oriented dataset was used in every experiment to assure consistency.

All the experiments were run on the same hardware: AMD Ryzen 3900X processor, Silicon Power 512GB NVMe A80 SSD drive and HyperX 2x16GB 3200MHz CL16 Fury RAM memory. Minimum background processes were running to avoid affecting runtime which was one of the metrics used in experiments.

Hierarchical binary classification vs multiclass approach

Application of the basic (2-class) CSP filters in our three-class problem, required using the hierarchical approach (first classifying the input state into rest/imagery movement, and then – if an imagery movement state was detected – it was further classified into left or right imagery hand movement). Multiclass CSP filters, however, enabled us to simplify the classification procedure.

The first group of experiments was conducted with 10 channel configuration, LDA classifier and 9-14Hz band-pass filter. The obtained results are presented in Fig. 5 (subject classification accuracy score), Table 1 (combined accuracy of each model), Table 2 (accuracy score broken down into individual classes) and Table 3 (time required for training/testing the models).

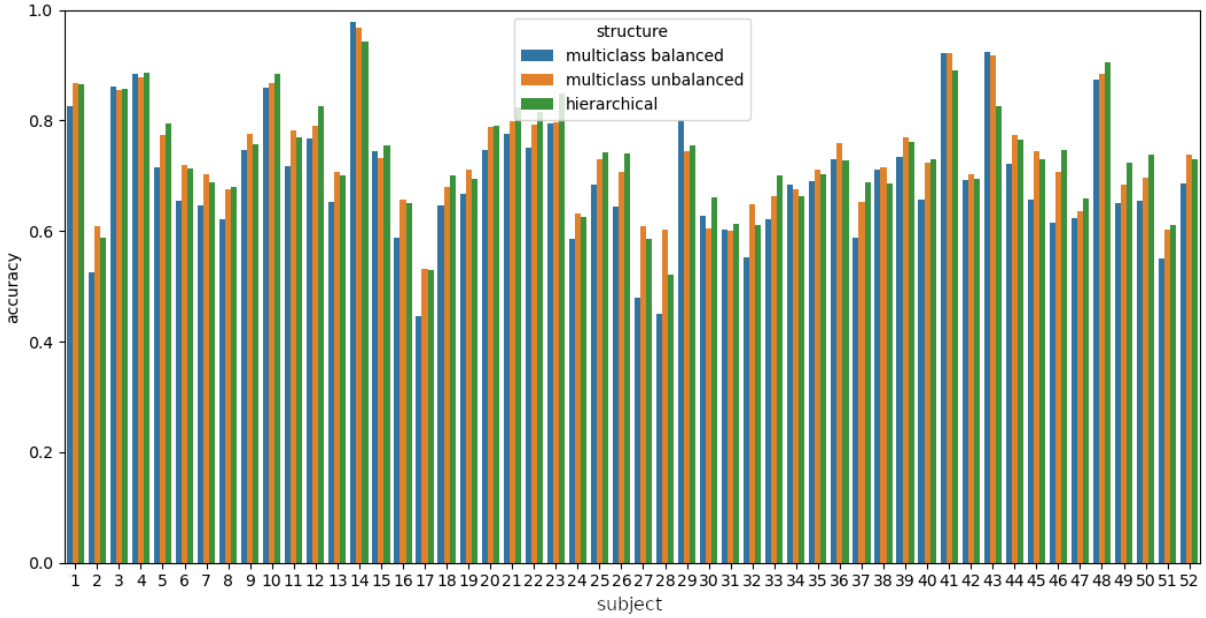

Figure 5. Subject classification accuracy for hierarchical, multiclass balanced and multiclass unbalanced model structure.

Table 1. Combined classification accuracy for hierarchical, multiclass unbalanced and multiclass balanced models.

Model	Accuracy
Hierarchical	0.7
Multiclass unbalanced	0.693
Multiclass balanced	0.687

Table 2. Classification accuracy broken down over class for hierarchical, multiclass unbalanced and multiclass balanced models.

Model	Rest accuracy	Left accuracy	Right accuracy	Left and Right accuracy
Hierarchical	0.832	0.637	0.628	0.633
Multiclass unbalanced	0.872	0.609	0.576	0.593
Multiclass balanced	0.807	0.649	0.622	0.636

Table 3. Average train and test runtime for hierarchical, multiclass unbalanced and multiclass balanced models.

Model	Train runtime	Test runtime
Hierarchical	0.405s	0.0139s
Multiclass unbalanced	0.316s	0.0073s
Multiclass balanced	0.248s	0.00563s

LDA and MLP classifiers

In the second group of experiments, two classifiers were used on top of the CSP filter-based preprocessing: LDA and a multilayer perceptron. MLP was trained using *Adam* optimizer with a constant learning rate of 0.001 and 1000 maximum iterations. This experiment was conducted on the multiclass balanced model with 10 channels and 9-14Hz band-pass filter. Subject classification accuracy score is shown in Fig. 6, combined accuracy in Table 4 and average runtime in Table 5.

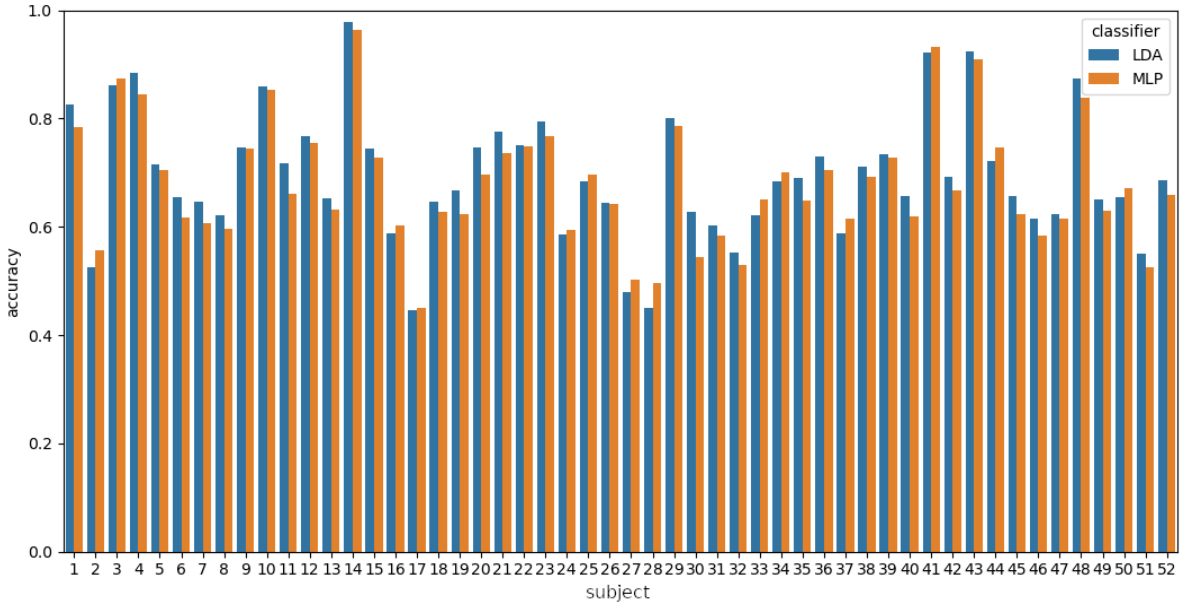

Figure 6. Subject classification accuracy comparison for LDA and MLP classifiers.

Table 4. Combined classification accuracy for LDA and MLP classifiers.

Classifier	Accuracy
LDA	0.693
MLP	0.679

Table 5. Average train and test runtime for LDA and MLP classifiers.

Classifier	Train runtime	Test runtime
LDA	0.24s	0.00599s
MLP	1.04s	0.0057s

Frequency band selection

The third group of experiments comprised classification tests with three different band-pass filters limiting the frequency range of the input EEG signal to 9-14Hz (potentially containing *mu* band ERD and ERS), 19-25Hz (potentially containing lower *beta* band ERDs and ERSs) and 6-30Hz (potentially containing both *mu* and lower *beta* ERDs and ERSs). This experiment was conducted on the multiclass balanced model with 10 channels and the LDA classifier. Accuracy classification metric was used for the evaluation of the results. No runtime experiments were performed for various band-pass filters, as there is obviously no difference in computational complexity between them. Subject classification accuracy score is shown in Fig. 7 and combined accuracy – in Table 6.

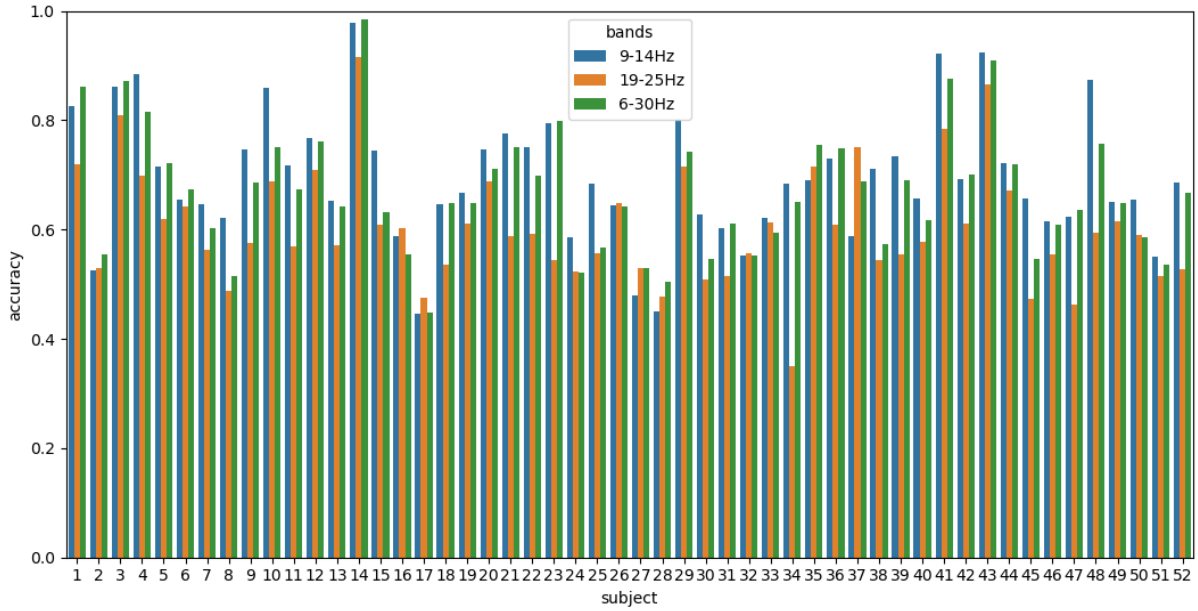

Figure 7. Subject classification accuracy comparison for 9-14Hz, 19-25Hz and 6-30Hz bands.

Table 6. Combined accuracy for 9-14Hz, 19-25Hz and 6-30Hz.

Band	Accuracy
9-14Hz	0.693
19-25Hz	0.603
6-30Hz	0.668

Channel selection

Four different channel configurations (2, 10, 18 and 64 channels) were compared in the fourth group of tests. This experiment was conducted on the multiclass balanced model with 9-14Hz band-pass filter and the LDA classifier. Subject classification accuracy score is shown in Fig. 8, combined accuracy results in Table 7 and average runtime in Table 8.

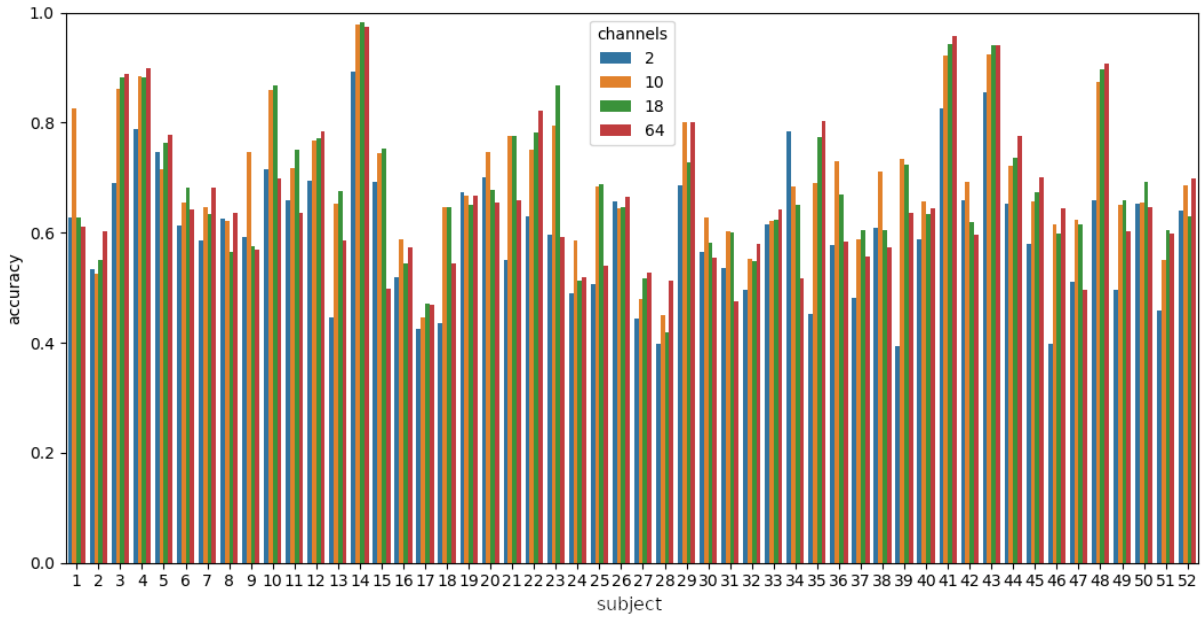

Figure 8. Subject classification accuracy for 2, 10, 18 and 64 EEG channels.

Table 7. Combined classification accuracy for 2, 10, 18 and 64 EEG channels.

Channel set (identified by channel count)	Accuracy
2	0.598
10	0.693
18	0.683
64	0.657

Table 8. Average train and test runtime for 2, 10, 18 and 64 EEG channels.

Channel set (identified by channel count)	Train runtime	Test runtime
2	0.035s	0.00135s
10	0.24s	0.00609s
18	0.501s	0.00683s
64	6.4s	0.0124s

Combined best model

To achieve the best results, the multiclass balanced model was selected. The data from 10 EEG channels was filtered with 9-14-Hz band-pass filter, preprocessed with 10 CSP filters and subjected to the classification procedure with LDA. Patient classification accuracy scores are shown in Fig. 9 and Table 9 presents the accuracy for the individual classes. Overall accuracy was 69.3%.

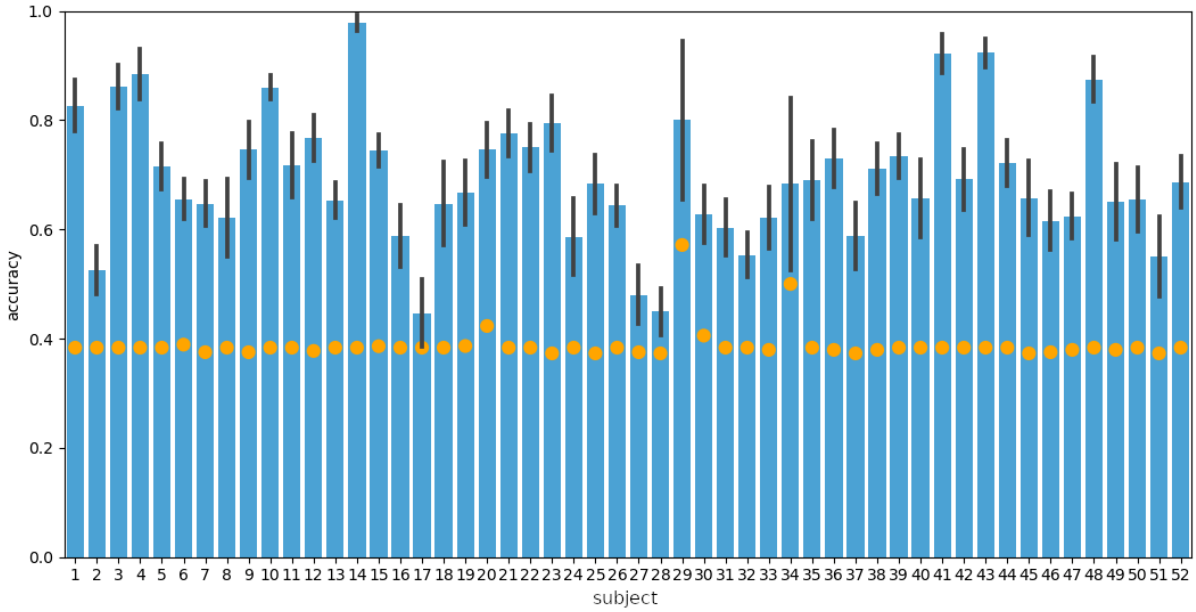

Figure 9. Subject classification accuracy for the best model. Standard deviation is presented by vertical grey bars and 5% best chance results are shown by orange dots.

Table 9. Classification accuracy with respect to the class.

Class	Accuracy
Rest state	0.807
Left-hand imagery movement	0.649120
Right-hand imagery movement	0.621750

DISCUSSION

Hierarchical and both multiclass models achieved significantly better classification accuracy scores for the rest state (83,2%, 87.22% and 80.7% respectively) than for the left/right movement (63.3%, 59.3% and 63.6% respectively). The balanced multiclass model obtained the highest accuracy on imagery movement classes (63.6%), but only slightly better than other models (63.3% and 59.3%). The balanced multiclass model was also the one that learned and produced results in the shortest time (0.248s/0.00563s vs 0.405s/0.0139s for hierarchical and 0.316s/0.0073s for multiclass unbalanced model). The implemented hierarchical model has its structure tied up to how the dataset was prepared. Using this model for another dataset with, for example, additional imagery leg movement examples, would require some significant changes.

LDA and MLP classifiers achieved similar accuracy scores (69,3% and 67.9%), proving that the simpler LDA classifier is enough for this classification task. The LDA classifier produced results in a similar time to the MLP classifier (0.00599s vs 0.0057s) but learned four times faster (0.24s vs 1.04s), which may be treated as an important advantage, especially in therapeutic scenarios involving re-training of the classifier in real-time.

Three frequency bands were selected, based on ERD/ERS characteristics typical for motor imagery events. As it turned out, the best overall accuracy score was achieved for 9-14Hz band (69.3%) followed by 6-30Hz band (66.8%) and – with noticeably worse accuracy

score – 19-25Hz band (60.3%). It is worth noting, that the classification accuracy score for some of the patients (17, 26, 27, 32 and 37 in Fig. 7) was higher in lower *beta* band than in the other bands. Further improvement could be achieved by selecting even narrower frequency bands on a per-subject basis, as suggested by Rosipal, Rošťáková and Trejo (2022).

Choosing only 2 channels was not enough (only 59.8% accuracy), either due to the lack of re-referencing possibilities or failing to precisely place the electrodes exactly over the target hand movement motor cortex part. Choosing 10 and 18 channels yielded comparable classification results (69.3% vs 68.3%) and test runtime. However, twice shorter training time (0.24s vs 0.501s) made 10 channel configuration a better choice.

CONCLUSIONS

In this paper, a solution was proposed for three-class (rest, left imagery hand movement, right imagery hand movement) classification that scored 68.9% accuracy in near real-time (training in 0.248s and producing results in 0.00563s). The proposed hierarchical model, although achieving the highest overall accuracy, was slower, more complex and less accurate for left/right imagery movement classes than the multiclass model. A less complex LDA classifier achieved comparable results to a much more complicated MLP classifier while learning 4 times faster. 9-14Hz band-pass filtering yielded better accuracy than 19-25Hz and 6-30Hz bands, proving that the *mu* band is the best one to use for motor imagery task classification. Channel configurations with more than 10 electrodes increased runtime significantly and did not improve accuracy. The conducted experiments and the resulting EEG classification model configuration will serve as a strong base for future works involving BCI-based VR environment design and implementation.

REFERENCES

Alhaddad, M. J. (2012). Common average reference (CAR) improves P300 speller. *International Journal of Engineering and Technology*, *2*(3), 21.

Cattan, G., Andreev, A., & Visinoni, E. (2020). Recommendations for integrating a P300-based brain–computer interface in virtual reality environments for gaming: an update. *Computers*, *9*(4), 92.

Cho, H., Ahn, M., Ahn, S., Kwon, M., & Jun, S. C. (2017). EEG datasets for motor imagery brain–computer interface. *GigaScience*, *6*(7), gix034.

Decety, J. (1996). Do imagined and executed actions share the same neural substrate?. *Cognitive Brain Research*, *3*(2), 87-93.

Dura, A., & Wosiak, A. (2021). EEG channel selection strategy for deep learning in emotion recognition. *Procedia Computer Science*, *192*, 2789-2796.

Grosse-Wentrup, M., & Buss, M. (2008). Multiclass common spatial patterns and information theoretic feature extraction. *IEEE Transactions on Biomedical Engineering*, *55*(8), 1991-2000.

Kaplan, A. Y., Shishkin, S. L., Ganin, I. P., Basyul, I. A., & Zhigalov, A. Y. (2013). Adapting the P300-based brain–computer interface for gaming: a review. *IEEE Transactions on Computational Intelligence and AI in Games*, *5*(2), 141-149.

Lécuyer, A., Lotte, F., Reilly, R. B., Leeb, R., Hirose, M., & Slater, M. (2008). Brain-computer interfaces, virtual reality, and videogames. *Computer*, *41*(10), 66-72.

Liao, L. D., Chen, C. Y., Wang, I. J., Chen, S. F., Li, S. Y., Chen, B. W., ... & Lin, C. T. (2012). Gaming control using a wearable and wireless EEG-based brain-computer interface device with novel dry foam-based sensors. *Journal of neuroengineering and rehabilitation*, *9*(1), 1-12.

Opałka, S., Stasiak, B., Szajerman, D., & Wojciechowski, A. (2018). Multi-channel convolutional neural networks architecture feeding for effective EEG mental tasks classification. *Sensors*, *18*(10), 3451.

Pfurtscheller, G., & Da Silva, F. L. (1999). Event-related EEG/MEG synchronization and desynchronization: basic principles. *Clinical Neurophysiology*, *110*(11), 1842-1857.

Rosipal, R., Rošťáková, Z., & Trejo, L. J. (2022). Tensor decomposition of human narrowband oscillatory brain activity in frequency, space and time. *Biological Psychology*, *169*, 108287.

van de Laar, B., Gürkök, H., Bos, D. P. O., Poel, M., & Nijholt, A. (2013). Experiencing BCI control in a popular computer game. *IEEE Transactions on Computational Intelligence and AI in Games*, *5*(2), 176-184.

Wojciechowski, A., Wiśniewska, A., Pyszora, A., Liberacka-Dwojak, M., & Juszczyk, K. (2021). Virtual reality immersive environments for motor and cognitive training of elderly people–a scoping review. *Human Technology*, *17*(2), 145-163.

Zhang, J., Yan, C., & Gong, X. (2017, October). Deep convolutional neural network for decoding motor imagery based brain computer interface. In *2017 IEEE international conference on signal processing, communications and computing (ICSPCC)* (pp. 1-5). IEEE.

Authors' Note

All correspondence should be addressed to
Stanisław Zakrzewski
Lodz University of Technology,
Łódź, Poland
Email stanislaw.zakrzewski@dokt.p.lodz.pl

Human Technology
ISSN 1795-6889
https://ht.csr-pub.eu